Long Fall Boots: A Proof of Concept for Reducing Joint Torques During Landing

Margaret Coad, Tony DiBlasi, Laura Hallock, and Christopher Merian
MAS.600 Human 2.0 - Massachusetts Institute of Technology

***Abstract*—In this study, a passive lower leg exoskeleton, consisting of a linear damper in parallel with the ankle, was designed to increase safety during a two-foot landing through the reduction of joint torque. Computational modeling aided in both the design of the device's geometry to optimize for desired output torque (100–200 Nm about each ankle) and the establishment of a kinematic landing model. Subjects dropped from a height of 0.71 m while wearing the exoskeleton with no damping (k = 0), low damping (k = 0.24 Ns/m) and high damping (k = 0.62 Ns/m) while motion capture data including joint angles, joint torques, and ground reaction force data was recorded. Chosen metrics for device success included resultant joint torque about the ankle and knee, as well as peak ground reaction force and time to peak ground reaction force. Results indicated that the low damping case decreased peak ankle torque by 12% and the high damping case decreased peak ankle torque by 30% as compared with the no damping case. Additionally, there was a 1% increase in time to peak ground reaction force for the low damping case and a 15% increase in time to peak ground reaction force for the high damping case. These results are encouraging, indicating that the device indeed made landing safer.**

***Index Terms*—landing, falling, jumping, lower-limb biomechanics, human dynamic modeling**

I. Introduction

A. Motivation

The human body is limited in its ability to land safely from even modest heights. Many lower extremity injuries, such as ACL tears and ankle sprains, are the direct result of the excessive impact of landing. As the foot initiates contact with the ground, the muscles and joints must absorb energy in order to slow the fall of the body's center of mass. Injuries occur when the impact velocity is too great or the joints are too stiff upon landing to transfer enough of the impact energy to the muscles.

The goal of this project was to design and test an exoskeleton that decreases the damage caused to the human body during landing. Based on a literature review, very little work has been done in this area: while many studies explore the effects of landing on the joints and describe different ways in which an athlete can be instructed to improve his or her safe landing ability, no studies were found that focus on the design of an exoskeleton to mitigate the risks associated with landing. A tangentially related device, called the PowerSkip (ALAN Sportartikel GmbH, Kottgeisering, Deutschland) has been shown to augment jumping ability, but it has not been reported as beneficial for landing. Thus, the device described in this paper is entirely new and innovative.

An exoskeleton that successfully reduces the risks of landing could be very useful. For example, firefighters and other emergency rescue personnel, who regularly enter unknown terrain and require agility and strength, could benefit from the increased athleticism provided by the device. Soldiers who jump from helicopters could use the device to prevent injury upon landing. Additionally, an exoskeleton like this could spark new recreational sports.

B. Approach

Because human landing is a biomechanically complex maneuver, involving several joints and many muscles, there exist many possible approaches to designing an exoskeleton to mitigate landing injury. Active and passive systems, springs and dampers, and augmentation of the ankle, the knee, and the hip were considered. Due to constraints on time and budget, a passive system that focused on a single joint and used one type of mechanical element was chosen.

The ankle was chosen as the joint to augment because, according to Devita and Skelly, the ankle plantarflexors absorb 44% of the energy of a drop landing, while the knee extensors and the hip extensors absorb 34% and 22%, respectively [1]. Since the most significant impact on the body's total energy absorption was desired, it was decided to augment the joint that already absorbs the largest amount of energy.

A damper was chosen rather than a spring because high torque is needed during the high velocity phase of landing, and the ankle already acts approximately like a spring, based on data from [1].

C. Hypothesis and Evaluation

The hypothesis postulated that adding a damper in parallel with the ankle would decrease the amount of torque that the ankle joint needs to provide, thus making landing safer for that joint. The primary measure of success was therefore whether the peak torque provided by the biological ankle during landing decreased.

II. Methods

A. Modeling

A dynamic model of the leg system was created to help understand the effects of adding a torsional damper to the ankle joint. This model was constructed in MATLAB (The MathWorks, Natick, MA) with a simplified representation of the leg system. The leg was modeled as a triple inverted pendulum with rigid links pinned to the ground and external forces at the top. The three links represented the foot, lower leg and upper leg, as shown in Fig. 1, which also shows the absolute limb angles and joint torques.

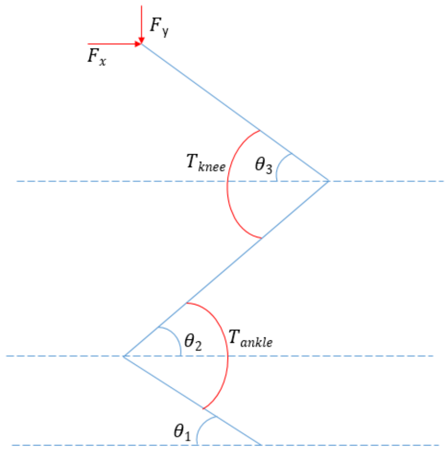

Fig. 1. Triple inverted pendulum layout. The foot, lower leg and upper leg angles are shown, as well as the ankle torque, knee torque and forces applied from the torso.

The data from [1], however, comprises only joint torques and relative angles, which cannot fully constrain the system. It was therefore necessary to add an absolute reference for the orientation of the pendulum. The external forces at the top of the inverted pendulum, located at the hip joint, were used to simulate the forces applied to the leg by the upper body during landing to avoid the necessity of modeling full body kinematics and dynamics. These external forces, however, were not supplied in the data, so they also needed to be added to create a complete system.

The dynamics of the system were calculated using Lagrange's equations of motion, with the three absolute limb angles as the generalized coordinates. These equations included the aforementioned inverted pendulum kinematics, as well as the torque and angle data from [1] and anthropometric leg

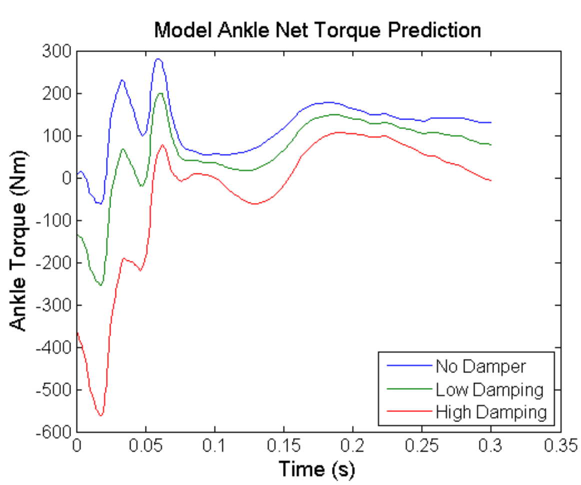

Fig. 2. Model-predicted ankle torque trajectories during landing. Plantarflexion torque is positive and time zero occurs when the foot touches the ground. The low and high damping coefficients match the damping coefficients used in experimentation.

size and inertia data from [2] and [3]. Since the data for joint angles from [1] was only angle position, which was created from a plot digitizer, it required significant conditioning to be usable. The data were smoothed significantly using a moving average filter (25 ms window) when calculating derivatives, as calculating acceleration from position proved extremely noisy without smoothing.

The Lagrangian equations generated a system of three differential equations for the absolute limb angles as a function of the remaining system parameters. This was rearranged to create a single differential equation for θ_1, the only free parameter when solving using the data in [1]. The other two equations were rearranged to calculate the unknown external forces, F_x and F_y. The differential equation for θ_1 was solved with MATLAB's `ode45` with estimated initial conditions; F_x and F_y were then calculated. After trying a few initial conditions, the θ_1 and $\dot{\theta_1}$ initial conditions were set to 40° and -90°/s. This gave a result that made sense, as the model touched down nicely over the landing period rather than penetrating the ground, a condition that was otherwise difficult to enforce given the model parameters.

With the θ_1 path and external forces defined, the model could now run with any three parameters free to be solved by the others as the differential equations progress through time. The three parameters chosen to be free were ankle torque, knee torque and ankle angle. This could be called "kinematic clamping," as the kinematics of the landing are largely fixed but the joint torques are free to vary. As seen in Fig. 2, the model predicts decreased peak plantarflexion (positive) as the torsional damper on the angle is increased.

This prediction does not fully correlate with intuitive expectations for the torque profile, as it indicates dorsiflexion (negative) torque applied briefly after touchdown, which becomes more negative as the higher damping applies more plantarflexion torque.

In the future, the model could also be used in other modes, such as "kinetic clamping," which would fix all the applied torques but leave the three joint angles free to vary. While this exploration was beyond the scope of this project, it could be useful in understanding how different landing trajectories evolve in time.

B. Design

1) Geometry: The most important device parameter was the ability to output 100–200 Nm of torque about the ankle on each leg during landing. Other essential design constraints included abiding by the geometry of the foot and shin, the stroke length of the chosen damper, allowing for safe range of movement, and reducing shear forces on the shin. A design with triangular geometry about the ankle was chosen (see Fig. 3) for easy manufacturing and to allow for the use of a linear damper, as appropriate torsional dampers were difficult to source.

A geometric model capable of calculating the output torque created by the damper during landing for a range of geometries (lengths A and B and angle Φ) was created in MATLAB. The

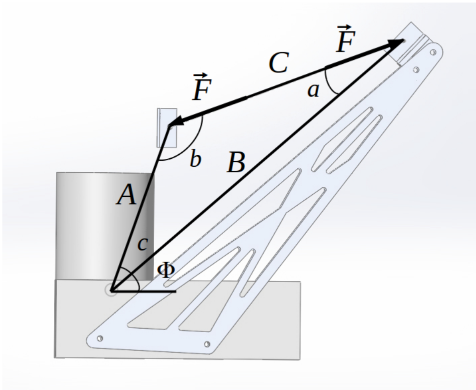

Fig. 3. CAD model of exoskeleton with relevant design parameters. Device was designed to provide maximum damping as close to normal to the surface of the shin as possible while obeying the geometric constraints of the lower leg.

damper force $\vec{F}$ shown in Fig. 3 generates torque about the rotation point of the ankle. The torque was calculated using the following equation:

$$\tau = F \cdot A \cdot \sin b \tag{1}$$

The model successfully generated a number of possible parameters that satisfied these geometry and torque constraints. One possible set of values — A = 0.20 m, B = 0.58 m, and Φ = 40° — was selected for ease of manufacturing.

2) Damper Selection: The linear damper selected for use was the McMaster-Carr 9899K91. This adjustable damper allowed for a 0.25 m stroke length and a maximum of 1200 N of force, more than sufficient for this use case.

3) Manufacturing: This exoskeleton was designed for ease of manufacturing and integration with the sole of a military combat boot. The support structures were cut with a water jet from 6061-T6 aluminum plate. Two identical aluminum panels were affixed on either side of the combat boot using bolts and spacing structures to ensure a parallel alignment. The aluminum panels were affixed at the upper point using a bracket and crossbar construction.

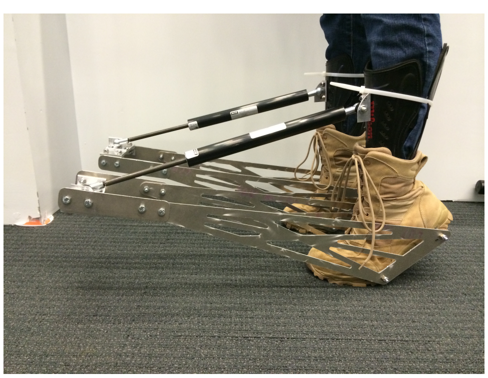

Fig. 4. Completed exoskeleton.

The damper was affixed to the device at the crossbar of the bracket at one end and to a shin guard at the other. The shin guard ensured the distribution of force on the shin at impact and allowed for control of length A along the shin.

Each completed structure had a mass of 1.9 kg and was worn by the subject by tightening the laces of the combat boot and fastening the shin guard securely to the shin. A second shin guard was then placed on the back of the lower leg and the two shin guards attached via zip ties to ensure that the damper remained affixed to the shin for the duration of each jump. The completed exoskeleton can be seen in Fig. 4.

C. Procedures

1) Test Subjects: Test subjects were selected to be athletic, in good health, and of a height and weight compatible with the damping forces modeled in our device design. A full data set was obtained from a male subject, 72.5 kg and 1.88 m in height, who exercised regularly as a member of the water polo team and had no known gait or movement pathologies. An incomplete data set was obtained from a second subject but was not used in further analysis.

2) Trial Parameters: Each jump trial consisted of a jump from a 0.71 m platform onto two stationary force plates. Subjects were instructed to push off with both feet when initiating the jump and to land on both feet as equally as possible. (This method was chosen over the more controlled step-off used in [1] because the weight and forces exerted by the device made stepping off the platform with one foot difficult. Additionally, examining the effects of different damping coefficients was more of interest than precisely controlling for jump height.) Test subjects were coached to refine an exact jump procedure over the course of the trials: subjects first stood at the edge of the platform with ankles slightly plantar flexed, applied additional plantar flexion to jump from the platform, and then landed — again with ankles slightly plantar flexed to avoid heel touchdown — with one foot on each of two force plates.

Ten jump trials were performed at each of two damper settings (0.24 Ns/m and 0.62 Ns/m), as well as ten trials in which the subject wore the device with the dampers detached as a control. The control trials were performed first, followed by those in which the lower damping coefficient was used, followed by those in which the highest damping coefficient was used, to allow the subject to acclimate to the bulky device and minimize injury.

Each subject was outfitted with a full set of reflective markers, and all trials were recorded using the MIT Media Lab Biomechatronics Group's Vicon motion capture system and force plates. All testing procedures were approved by the MIT Committee on Use of Human Experimental Subjects (COUHES).

3) Data Processing: Vicon motion capture data was labeled using the `HelenHayesSIMM3Biomech` skeleton model developed by the Biomechatronics Group, modified slightly to remove the medial elbow markers, which were not visible in the T-Pose trial used for labeling. Each trial was then auto-labeled and all trajectories manually gap-filled. The five most

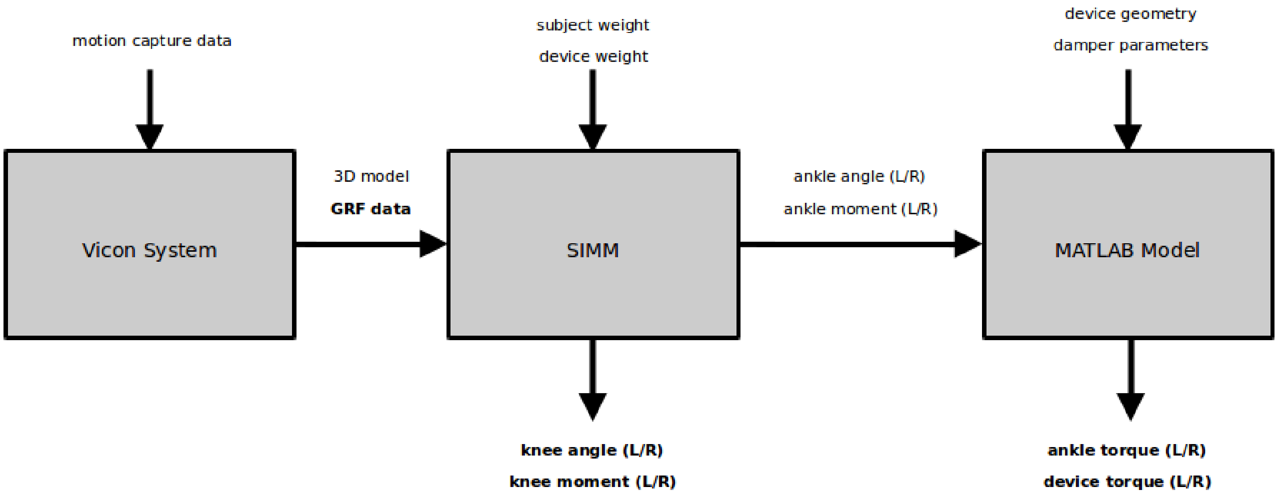

Fig. 5. Data analysis pipeline. Bold indicates datasets used in final analysis.

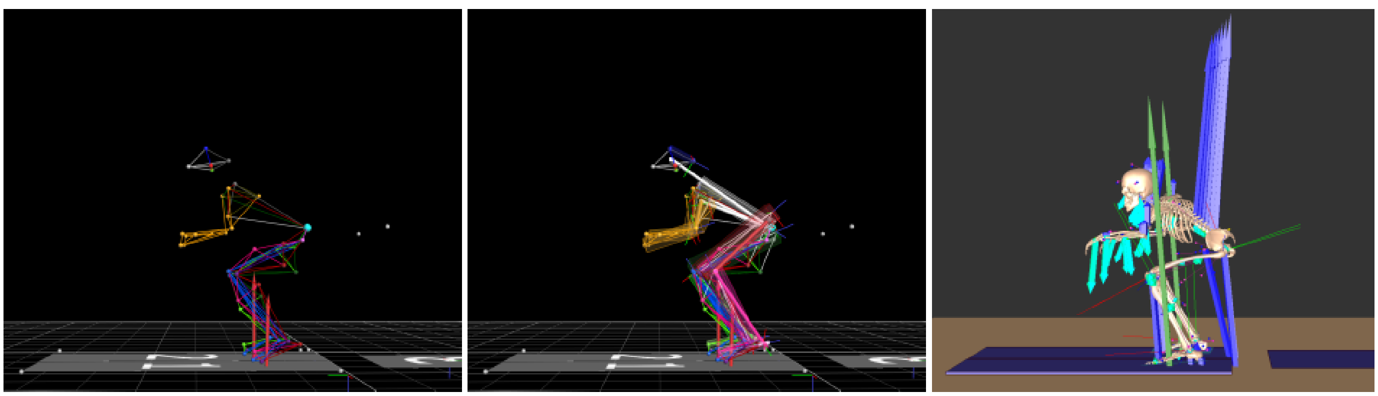

Fig. 6. Visual jump trial data from Vicon and SIMM. *Left*: Vicon skeleton between reflective markers. *Center*: Vicon solid model extrapolated from triangulation between markers. *Right*: Joint velocities calculated in SIMM.

complete trials at each damper setting were then passed to SIMM for further analysis.

Each trial was then processed in SIMM to calculate the full dynamics of each landing, including time trajectories of ankle angle, ankle moment, knee angle, and knee moment, for both left and right sides. The ankle angle and moment data were then processed through the MATLAB model of the device geometry to determine the moment exerted by the device and the moment exerted by the subject's ankle at each time step.

The data processing pipeline is further described in Fig. 5. Example jump trial visual data is shown in Fig. 6.

III. Results

A. Ankle Angle and Torque

The ankle angle trajectories were analyzed, along with their corresponding joint torques, for three scenarios: without the damper, with low damping, and with high damping. Note that the torque values presented here are for one ankle, not two. Fig. 7 shows a representative trace of both the ankle angle and the ankle torque versus time for a trial without the damper.

The zero point of ankle angle occurs when the subject is standing upright with feet flat. Correspondingly, ankle torque is defined as positive for plantarflexion and negative for dorsiflexion. Time zero is the time at which the subject's toes

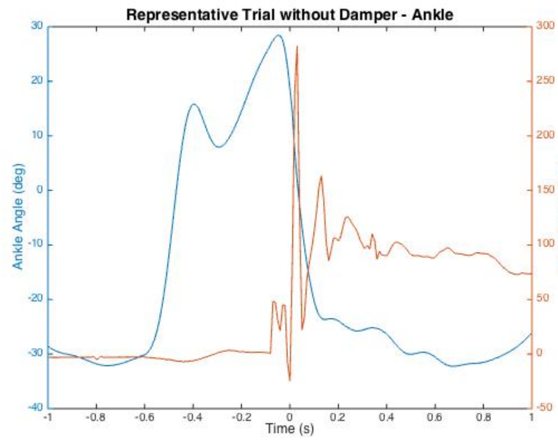

Fig. 7. Representative traces of ankle angle and ankle torque versus time with no damping. Plantarflexion is positive for both angle and torque, following the same convention used in initial modeling.

first touched the ground. Note that, at a time of around -0.6 s, the subject's ankle angle began increasing from -30° to +30° as the subject jumped off the platform. At time zero, the ankle angle then rapidly decreased as the subject landed and dorsiflexed. Note also that the ankle torque spiked immediately after time zero, as the subject's ankle began to absorb the energy of the landing. Finally, the ankle torque leveled off to the value needed to balance the weight of the subject's body in a squatting position.

Fig. 8 shows a comparison of representative traces of ankle torque versus time for the three scenarios described above. As described in §2.C.3, the torque provided by the damper was calculated using the MATLAB device geometry model. The damper torque profile was then subtracted from the total ankle torque trace measured by the Vicon system to obtain the trace for the torque required of the biological ankle. The resulting biological ankle torques are shown here.

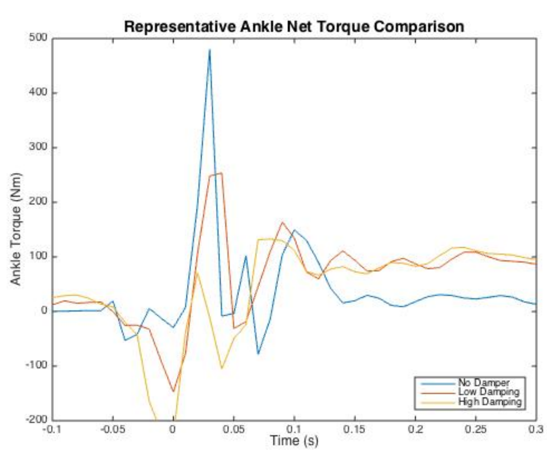

Fig. 8. Comparison of representative traces of ankle torque versus time for no damper, low damping, and high damping.

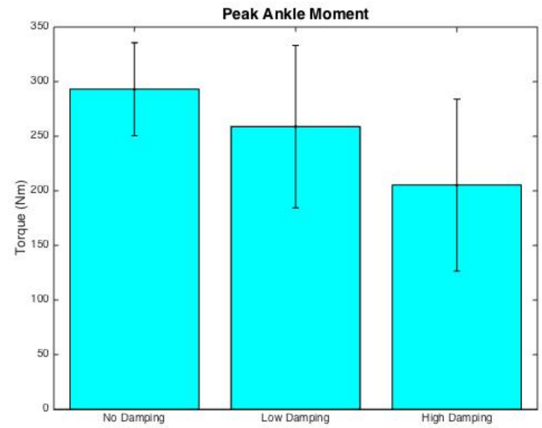

Fig. 9. Comparison of average peak ankle moment for the no damping, low damping, and high damping cases. Error bars show one standard deviation above and below the mean for this and subsequent figures.

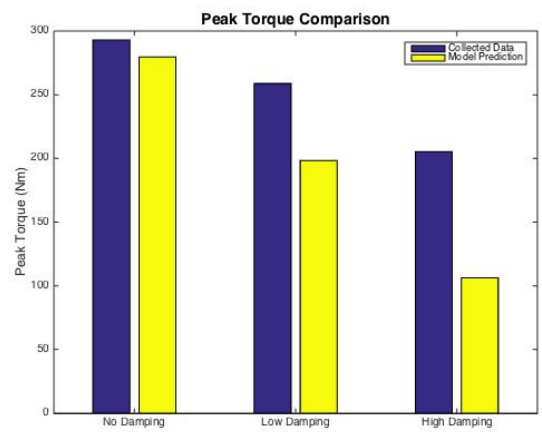

Fig. 10. Comparison of peak ankle torques as measured during the experiment and as predicted by the model.

Note that the peak positive ankle torque is different for the three representative traces shown in Fig. 8. The peak is the highest for the no damping case, and lowest for the high damping case. Fig. 9 focuses on this difference, as it shows the average peak ankle moment over the five trials for each damping setting. The error bars show one standard deviation above and below the mean value.

There is a clear trend in the average values of the ankle torque: the higher the damping, the lower the peak ankle torque. Compared with landing without any damping, the device with low damping decreased the peak ankle torque by 12%, and the device with high damping decreased the peak ankle torque by 30%.

B. Model Comparison

Fig. 10 shows a comparison of the peak ankle torques that were measured with those predicted by the model described above. The same trend is present between the data from the model and the data from the experiment, although the model predicted a more drastic change in ankle torque than was actually observed.

C. Knee Angle and Torque

Although the device surrounds only the ankle joint, it is worth observing how the device impacts other joints involved in human landing. Fig. 11 shows a representative trace of the knee angle and knee torque versus time without the damper. Knee angle and torque are defined as positive for extension and negative for flexion. Angle zero is defined as the knee angle when the subject is standing straight up. Again, these data are for a single knee, not two. At a time of around -0.6 s, the knee angle increases to almost 0° as the subject jumps and then quickly decreases to below -100° as the subject lands. Note also that the knee torque spikes at time zero and then levels off to the value required to hold the subject's body in the squatting position until the subject stands up.

Fig. 12 shows representative traces of the knee torque versus time for the three damping levels. Note that the differences between the traces in this case are less obvious.

Fig. 13 shows the average of the peak knee moments for each of the five trials for each damping setting. As compared with the no damping case, the device with low damping decreased the average peak knee torque by 3% and the device with high damping increased the average peak knee torque by 21%. The standard deviation, however, was notably higher than that of the other two data series.

D. Knee and Ankle Comparison

Fig. 14 shows a summary of the effect of the different damping coefficients on the peak ankle and knee torques. As the damping increased, there was a clear negative trend in the peak ankle torques and there was no observable trend in the peak knee torques.

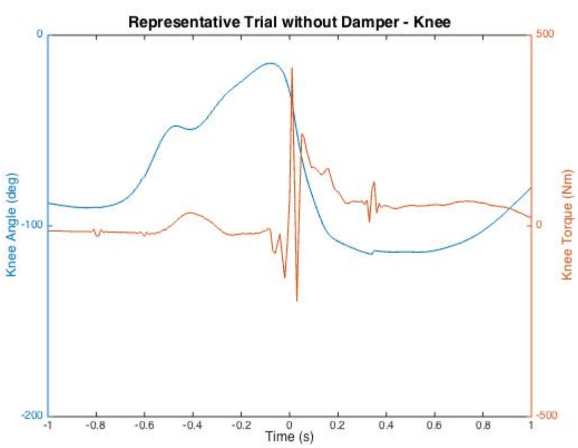

Fig. 11. Representative traces of knee angle and knee torque versus time with no damping.

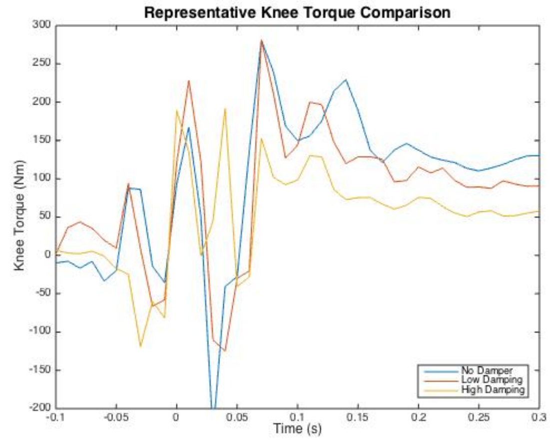

Fig. 12. Comparison of representative traces of knee torque versus time for no damper, low damping, and high damping.

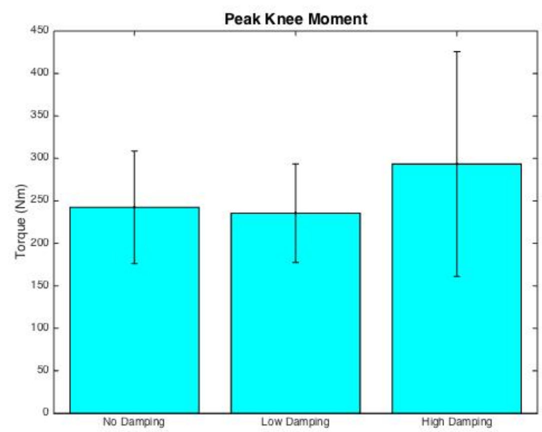

Fig. 13. Comparison of average peak knee moment for the no damping, low damping, and high damping cases.

E. Ground Reaction Forces

The ground reaction forces measured by the force plate were also analyzed. Note that these forces represent the force on the ground per leg. Fig. 15 shows a comparison between representative ground reaction force curves versus time for the three levels of damping. All ground reaction force traces had the same general shape, in which the force peaked approximately 10 ms after landing and then oscillated until it reached its steady state value, the force due to the weight of the subject.

Fig. 16 compares the peak ground reaction forces averaged over the five trials for each of the three damping values. As compared with the landing without any damping, the landing with the device on low damping increased the peak ground reaction forces by 11%, and with the device on high damping decreased the peak ground reaction forces by 1%.

Fig. 17 compares the time from initial contact to the peak ground reaction force as averaged over the five trials for the

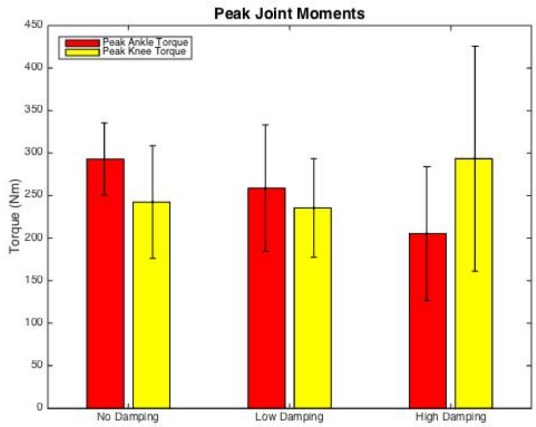

Fig. 14. Comparison of average peak ankle and knee torques for the three damping scenarios.

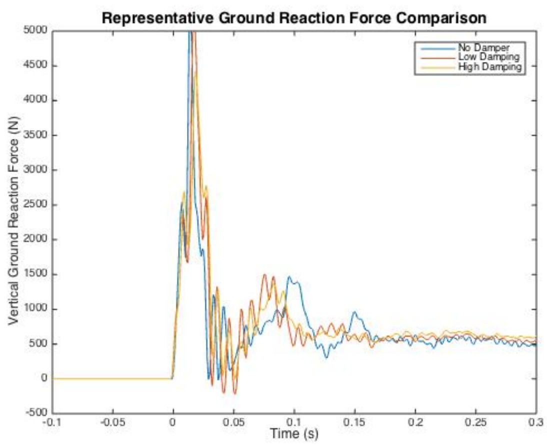

Fig. 15. Comparison between representative ground reaction traces for no damping, low damping, and high damping.

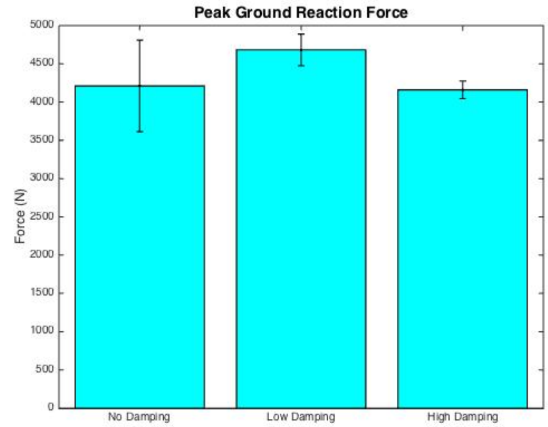

Fig. 16. Comparison of peak ground reaction forces for three damping values.

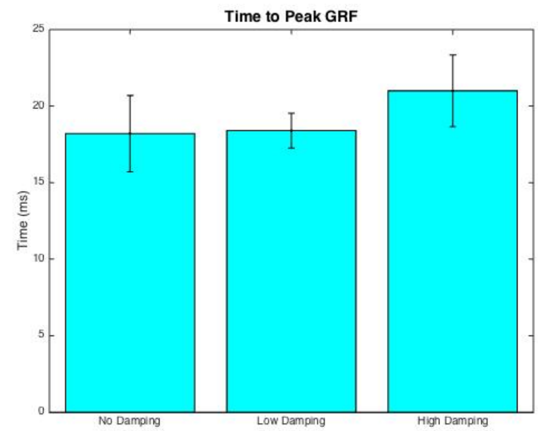

Fig. 17. Comparison of time to peak ground reaction force for the three damping values.

three damping coefficients. As compared with the landing with no damping, the landing with the device on low damping increased the time to peak ground reaction force by 1%, and the landing with the device on high damping increased the time to peak ground reaction force by 15%.

F. Qualitative Results

In addition to the quantitative results, the subjects were asked about their experiences wearing the device.

The first subject commented that jumping with the device without the damper attached "felt pretty normal . . . like jumping with a slight bit of [extra] weight away from [his] center of gravity."

Both subjects reported feeling a lot of force going into their shins with the device set on low damping, which took some getting used to. The second subject said that the forces felt in the ankle and foot did not feel very different from those without the damper. The first subject, on the other hand, commented that with the damping, "the ankle felt good."

Only the first subject had the opportunity to jump with the device set on high damping, and he reported that he did not feel any forces on his heels as he was landing with the device because his heels did not touch the ground — or, if they did, they only touched lightly. He also said that he felt landing forces that were lower in magnitude with the device set on high damping than without the damping.

Both subjects described a process of learning to use the device, which involved allowing the device to take the load and adjusting their normal landing position. The first subject reported that he "learned to land just on [his] toes and steady [himself] that way." Both subjects also commented that their shins felt slightly bruised from wearing the device. Their shins looked red after they took the device off, but no bruises were immediately visible.

G. Failure Modes

While a full set of data was obtained for the first test subject, during the second subject's low-damping trials, bending in the metal frame of the device was observed and trials were halted for the subject's safety. It is hypothesized that a major contributing factor to this device damage was the second subject's gait: unlike the first subject, who successfully executed two-foot jumps on each trial, the second subject had difficulty both jumping and landing on both feet equally, causing disproportionate stress on the inside aluminum plate on the left boot. Due to time constraints, the device was not rebuilt and no more data was acquired, but future designs should be robust to these pathologies.

IV. Discussion

A. Discussion of Results

This study focused on the creation of a simple ankle-based exoskeleton capable of reducing torques about the joints during a two-foot landing. This proof-of-concept device was tested using motion capture techniques and ground reaction force data to collect gross joint torques and angles for the ankle and knee while wearing the device. The net joint torques were then calculated by feeding the kinematic data into a geometric model and subtracting the torque output by the device from the gross torque. As a measure of efficacy, the resultant torques of the ankle, ground reaction forces, as well as time to peak ground reaction forces were analyzed for control (no damping), low damping (0.24 Ns/m), and high damping (0.62 Ns/m) scenarios.

The results indicated that, as the damping coefficient increased, there was a clear decrease in peak ankle torque from 293 Nm for no damping, to 259 Nm for low damping, to 203 Nm for high damping. This trend matched the kinematic modeling, though the exact peak magnitudes did not.

There was no trend relating changes in the peak knee torques or the peak ground reaction forces to increases in the damping coefficient. There was, however, a trend indicating that, as the damping coefficient increased, the time to peak ground reaction force increased from 18 ms for no damping to 21 ms for high damping. Puddle and Maulder [4] cited such increased time as a measure of improved landing performance.

B. Sources of Error

The primary sources of error in the data and device torque model are most likely the inherent assumptions made during the kinematic and device torque modeling process. The largest source of error is associated with the idealization of the damper. The damping coefficients for high and low damping were measured by observing the fall time of a known weight at a slow speed. Due to this rather simplistic measure, it is not possible to take into account non-linearities of the damper, nor ensure the accuracy of the damping coefficient at high speeds. A more thorough characterization of the damper at its expected operating conditions would allow for more precise modeling of the device torque over time. Ideally, this model could be eliminated altogether by directly measuring the torque exerted by the damper rather than estimating it based on the device geometry and ankle angle over time.

Additionally, the lengths of the device (lengths A, B, and C) are idealized in this device model. Shifting of the lengths, such as those caused by the slipping of the shin guard over the period of testing, introduces unmodeled deviation from the idealized lengths. This contribution to error is likely minimal but still impacts the torque calculation.

Lastly, the sophisticated modeling involved in the joint torque calculation from the Vicon/SIMM system intrinsically introduces error, as its solid model dynamics rely on average human morphological parameters that may not precisely match those of our subject. In future experimentation, direct measurements of the ankle torque and damper force with load cells could provide more accurate results.

V. Conclusion

The device described in this paper showed very promising results in that it successfully decreased the peak torque exerted by the biological ankle during landing. The device also increased the time to peak ground reaction force. Both of these measures indicate that the device improved the safety of landing while leaving knee torques and peak ground reaction forces almost unchanged.

In the future, this device could be expanded to other joints, such as the knee and the hip. Other possible directions of exploration include making the device more comfortable, robust to asymmetries in landing, and less obtrusive during activities such as walking and running.

Acknowledgments

We would like to thank the MIT Biomechatronics Group for their generous contribution of resources, time, and mentorship. A special thanks to Tyler Clites, Luke Mooney, and Michael Eilenberg for contributing their expertise and offering an incredible amount of insight throughout the project. We would also like to thank our test subjects, Brady Knight and Kyle Archer, for their time and cooperation.

References

[1] Paul Devita and William A. Skelly, "Effect of landing stiffness on joint kinetics and energetics in the lower extremity," *Medicine and Science in Sports and Exercise*, vol. 24. no. 1 (1992).

[2] Ernest Hanavan, "A Mathematical Model of the Human Body" (1964).

[3] P. Grimshaw and A. Burden, *Sport and Exercise Biomechanics*, p. 140, Taylor & Francis Group (2006).

[4] Damien Puddle and Peter Maulder, "Ground Reaction Forces and Loading Rates Associated with Parkour and Traditional Drop Landing Techniques," *Journal of Sports Science and Medicine*, vol. 12, p. 122-129 (2013).